

Orbital period variation in the chromospherically active binary FF UMa (2RE J0933+624)

M.C. Gálvez^{1,2}, D. Montes¹, M.J. Fernández-Figueroa¹,
E. De Castro¹ and M. Cornide¹

¹Department de Astronomía, Facultad de Físicas, Universidad Complutense de Madrid, in
Madrid, Spain
email: mcz@astrax.fis.ucm.es

²Department of Astronomy, University of Florida, Bryant Space Science Center, Gainesville,
Florida, USA
email: mcz@astro.ufl.edu

Abstract. We present here a detailed study of FF UMa (2RE J0933+624), a recently discovered, X-ray/EUV selected, active binary system with strong H α emission. By using high resolution echelle spectroscopic observations taken during five observing runs from 1998 to 2004, we derived precise radial velocities that allowed us to determine the orbital solution of the system at different epochs. Analyzing these orbital solutions and a previous one in 1993, determined by other authors, we have found a change in the heliocentric Julian date on conjunction (T_{conj}) that can be explained by a change with time in the orbital period of the system. The relative amplitude of the orbital period variation derived from these data was $dP/P \approx 5 \times 10^{-4}$, which results to be larger than the variations found in other similar chromospherically active binaries like AR Lac and HR 1099. This orbital period variation can be related (Applegate 1992; Lanza 1998 and Lanza 2006) with the modulation of the gravitational quadrupole-moment of its magnetically active secondary star produced by angular momentum exchanges within its convective envelope. In addition, using these observations, we have determined the stellar parameters of the components and we have carried out a study of the chromospheric activity using all the optical indicators from Ca II H&K to Ca II IRT lines.

Keywords. stars: binaries: spectroscopic, stars: activity, stars: atmospheres, stars: chromospheres, stars: late-type, stars: fundamental parameters

1. Observations

The spectroscopic observations of this binary system were obtained during five observing runs from 1998 to 2004:

- 12 to 21 January 1998 using the 2.1 m Otto Struve Telescope at McDonald Observatory Texas (USA) with the Sandiford Cassegrain Echelle Spectrometer. During this observing run, a 1200x400 pixel CCD detector was used. The spectrograph setup was chosen to cover the H α (6563 Å) and Ca II IRT (8498, 8542, 8662 Å) lines. The wavelength range covers from 6400 to 8800 Å in 31 orders. The reciprocal dispersion ranges from 0.06 to 0.08 Å/pixel and the spectral resolution, determined as the FWHM of the arc comparison lines, ranges from 0.13 to 0.20 Å. In one of the nights, we changed the spectrograph setup to include the He I D₃ (5876 Å) and Na I D₁, D₂ (5889.9, 5895.9 Å), with wavelength coverage of 5600-7000 Å.
- 22 to 24 January 2000 using the 9.2 m Hobby-Eberly Telescope (HET) at McDonald Observatory Texas (USA), with the medium resolution spectrograph UFOE (Upgraded Fiber Optic Echelle). A 1200x400 pixel CCD detector was used. The wavelength range

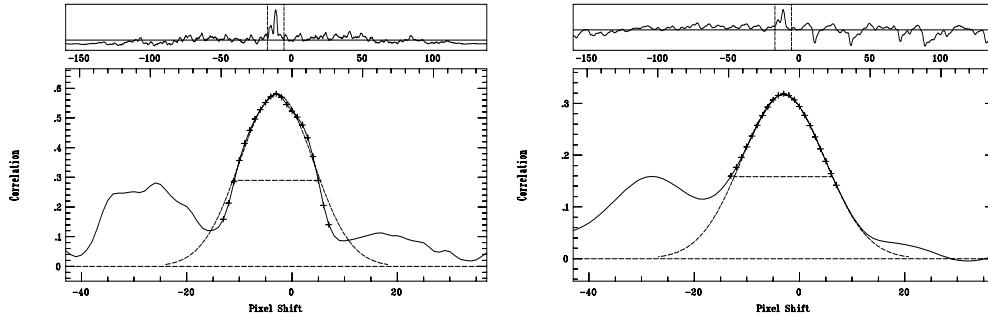


Figure 1. Cross-correlation functions (CCFs) of the both components of the binary system, fitted with Gaussians. (a) left panel, original CCF, (b) right panel, corrected CCF.

covers from 4400-9150 Å in 26 orders. The reciprocal dispersion ranges from 0.06 to 0.17 Å/pixel and the spectral resolution (FWHM) from 0.14 to 0.42 Å.

- April 2002 and April 2004. These observing runs took place on 22 to 26 April 2002 and from 29 March to 7 April 2004, using the 2.2 m telescope at the German Spanish Astronomical Observatory (CAHA) (Almeria, Spain). The Fibre Optics Cassegrain Echelle Spectrograph (FOCES) was used with a 2048² 24μ SITE#1d CCD detector. The wavelength range covers from 3450 to 10700 Å in 112 orders. The reciprocal dispersion ranges from 0.04 to 0.13 Å/pixel and the spectral resolution (FWHM) ranges from 0.08 to 0.35 Å.

- This run was made on 2 to 6 April 2004, using the 2.56 m Nordic Optical Telescope (NOT) located at the Observatory Roque de Los Muchachos (La Palma, Spain). The Soviet Finnish High Resolution Echelle Spectrograph (SOFIN) was used with an echelle grating (79 grooves/mm), ASTROMED-3200 camera and a 20522 pixel 2K3EB PISKUNOV1 CCD detector. The wavelength range covered is from 3545 to 10120 Å in 42 orders. The reciprocal dispersion ranges from 0.033 to 0.11 Å/pixel and the spectral resolution (FWHM) from 0.14 to 0.32 Å.

2. Radial velocities

Heliocentric radial velocities of both components have been determined by using the cross-correlation technique. The spectra of the program stars were cross-correlated order by order, using the routine FXCOR in IRAF, against spectra of radial velocity standards of similar spectral types. The velocity is derived from the position of the cross-correlation peak (Figs. 1a, b). As the system is SB2 we can see two peaks in the CCF coming from the two components and we can fit each peak separately. When the components are too close, we used deblend fits. But as it can be seen in the Fig. 1a the irregular profiles (double peaks and asymmetries) can produce errors in radial velocity measures. To correct this error, we recalculated the radial velocities using the cross-correlation technique against spectra of the same radial velocity standard star but rotational broadened to the rotational velocity of the components of FF UMa ($v \sin i \approx 30 \text{ km s}^{-1}$). This way the profiles of CCF become regulars, see Fig. 1b.

3. Orbital Period Variation

With 39 radial determined by us (from 1998 to 2004) and 9 given by Jeffries et al. (1995), we tried to compute the orbital solution but we find some tricking facts. When

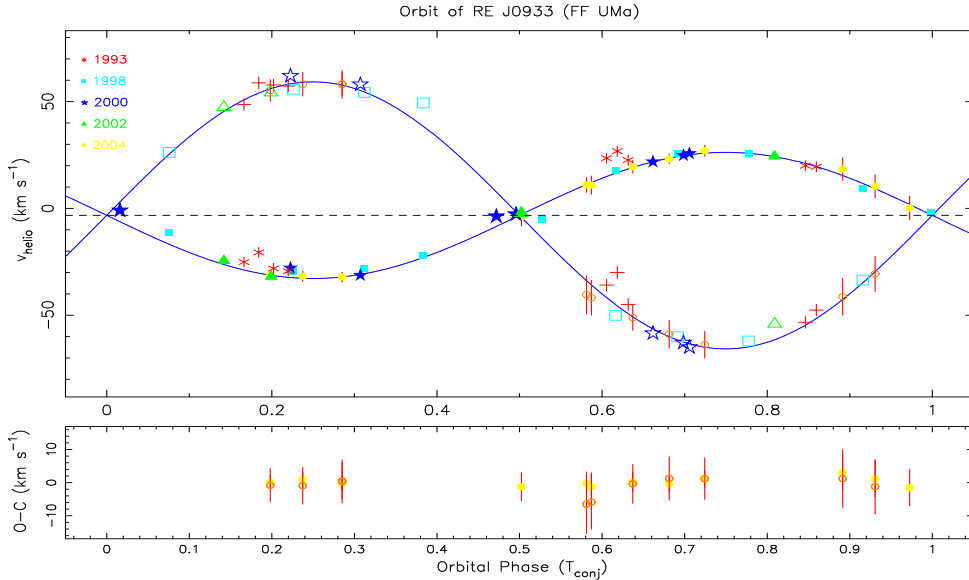


Figure 2. Radial velocities of all observing runs. We plotted the orbital solution (continuum line) of the FOCES04 observing run and we have superimposed the data from the rest runs shifted in phase according with the determined O-C in T_{conj} , see text for explanation. Different symbols and colours correspond to different epochs (1993 (Jeffries 1995), and 1998 - 2004 our observing runs).

Table 1. Orbital solution

Element	Value	Uncertainty	Units
P_{orb}	3.274	0.054	days
T_{conj}	53090.84	0.18	HJD (2400000 +)
ω	0.00	0.00	degrees
e	0.00	0.00	(adopted)
K_1	29.55	0.95	km s^{-1}
K_2	62.52	3.60	km s^{-1}
γ	-3.23	0.77	km s^{-1}
$q = M_1/M_2$	2.12	0.10	
$a_1 \sin i$	1.330	0.048	10^6 km
$a_2 \sin i$	2.81	0.17	10^6 km
$a \sin i$	4.14	0.18	10^6 km
"	0.028		AU
"	5.95		R_{\odot}
$M_1 \sin^3 i$	0.180	0.024	M_{\odot}
$M_2 \sin^3 i$	0.085	0.012	M_{\odot}
$f(M)$	0.00875	0.00099	M_{\odot}

we fit the data from each observing run separately we obtain a good orbital solution, but when we tried to fit the total orbital solution (using all the radial velocities from the different epochs) we are not able to find a good orbital solution. Analyzing in detail these results we discover that orbital parameters obtained at different epochs are very similar, but there is a shift in the heliocentric Julian date on conjunction (T_{conj}). See Figs. 2 and 3.

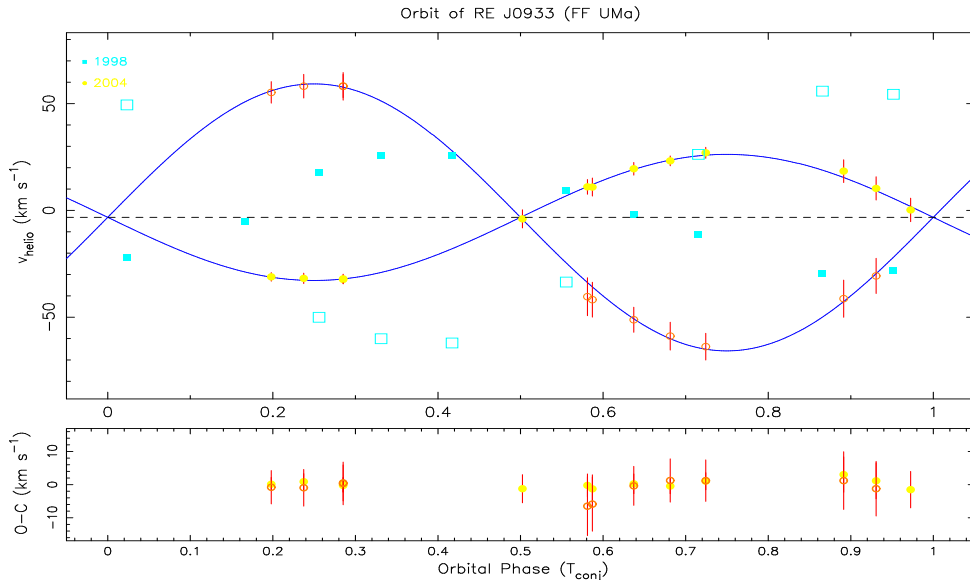


Figure 3. Note the orbital phase shift between the orbital solution with the data of the FOCES04 observing run (continuous line) and McDonald 1998 (blue squares)

Taken this into account, we computed the orbital solution with the FOCES04 run and shifted in phase the rest of the observing runs (see sect. 4). We have analyzed the different hypothesis that can explain this behaviour:

- The existence of another star as a distant third component of the system could introduce changes in the main orbit of the observed system. Variations in the center of mass radial velocity (γ) could indicate the presence of a third component (Cumming 2004). However, the amplitude of the variations in γ we have found in our data is only of 3 km s^{-1} .

- The presence of photospheric starspots in the active components of this binary, could produce asymmetries in the absorption line profiles and the corresponding CCF. This could affect the radial velocity data and this way transmit errors to the orbital solutions. However, we have found (see sect. 2) that this is not the case.

- Another explanation associated to the magnetic activity could be an orbital period modulation due to the variation of activity with time. It can be explained as a consequence of cyclic variations of the quadrupole-moment of both components of the system along the magnetic activity cycle. In the study of the RS CVn system HR 1099, Frasca & Lanza (2005) based on the hypothesis presented by Matese & Whithmore (1983) and elaborated later by Applegate (1992) and Lanza et al. (1998), in which temporal variations of some RS CVn systems could be due to changes in the quadrupole-moment of primary component along the activity cycle and that come from the exchange between kinematics and magnetic energy driven by the stellar hydromagnetic dynamo. The results obtained until this study were variations of $dP/P \approx 10^{-6}$ - 10^{-5} in an interval of 7 to 109 years. In FF UMa we have found a variation of $dP/P \approx 10^{-4}$ in 11 years, one order of magnitude higher, but it could be explained by the higher efficiency of the dynamo mechanism in the components of the system.

In Table 2 we present the orbital period variation deduced from the orbital solution of the different observing runs, in the first column we give the year of the observing run, in the second, T_{conj} , in the third, the O-C (Observed - Calculated = difference between

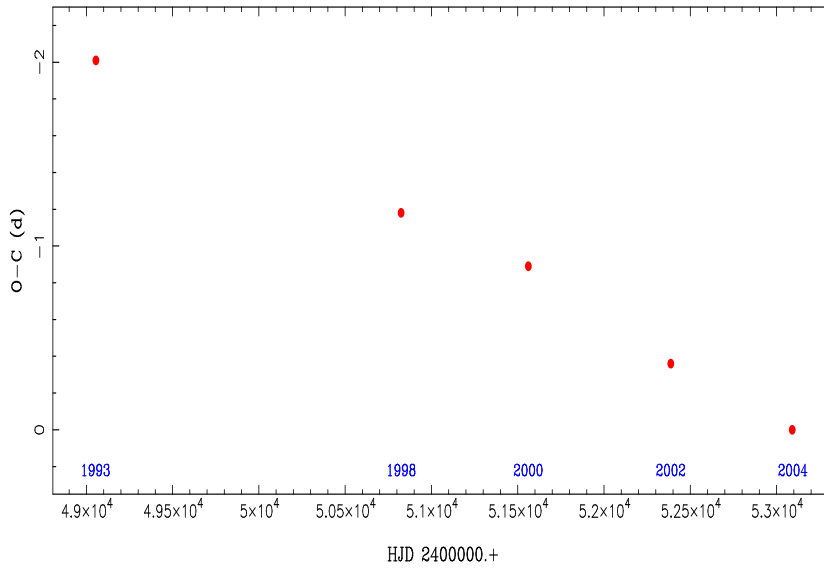


Figure 4. Period variation representation. The difference (O-C) is plotted against Heliocentric Julian date HJD for every observing run.

Table 2. Variations of Orbital Period (P)

Year	T_{conj} HJD (2400000 +)	O-C day	dP/P
1993	49055.8789	-2.0089	4.979×10^{-4}
1998	50824.4023	-1.1755	5.187×10^{-4}
2000	51561.2227	-0.9005	5.887×10^{-4}
2002	52386.6758	-0.3615	5.134×10^{-4}
2004	53090.8398		

the observed T_{conj} , and calculated T_{conj} , from the FOCES04 run that has been taken as reference), and in the last column the relative orbital period variation, dP/P . Fig. 4. represents the variation of the O-C (T_{conj}) for every run with time. The amplitude of the variation is 2 days and it look like a linear tendency. We would need a larger time observation for testing if the tendency remains linear or becomes sinusoidal as it is expected if there is a cycled motion.

Although recent studies, as Lanza (2006), are not completely in agreement with Aplegate model, we found that the quantitative explanation of the phenomena is the most likely for FF UMa system.

4. Orbital Solution

We have computed the orbital solution of this system using radial velocities data of FOCES 2004 observing run. The radial velocity data are plotted in Fig. 2. Solid symbols represent the primary and open symbols represent the secondary and each observing run is represented in a different symbol. The curve represent a minimum χ^2 fit orbit solution. The orbital solution and relevant derived quantities are given in Table 1 and Fig. 2. In this table we give T_{conj} as the heliocentric Julian date on conjunction with the hotter star

behind, in order to adopt the same criteria used in previous papers. We have obtained a circular orbit with a orbital period of about 3.274 days. As $P_{\text{phot}} \approx 3.270$ days we can say that it is a synchronous system. The mass ratio is about 2.12 concluding that the components are very different. The values of parameters are in agreement with Jeffries et al. (1995).

5. Chromospheric Activity

The chromospheric contribution in the different optical chromospheric activity indicators has been determined using the spectral subtraction technique Montes et al. (1995; 1997; 1998). The synthesized spectrum was constructed using the program STARMOD developed at Penn State (Barden 1985). We have deblended the emission from both components using a two-Gaussian fit except for the $H\alpha$ line. The profiles of the $H\alpha$, and Ca II IRT ($\lambda 8498$, $\lambda 8542$) lines are plotted in Fig. 5. For each observation we have plotted the observed spectrum (solid-line) and the synthesized spectrum (dashed-line) in the left panel and the subtracted spectrum (dotted line) in the right panel. The $H\alpha$ line of both components is observed always in emission above the continuum in the observed spectra (see Fig. 5 *a*). This emission is persistent during all the observations indicating that it is a very active binary system similar to some RS CVn and BY Dra systems.

Measuring the EW of this line, we found that each star of the system have a broad component that avoid to fit the emission lines with only one Gaussian. We could not fit the emission lines with four Gaussian components (two, narrow and broad components, for each star). The best fit is obtained when we use a Lorentzian profile for each component (see Fig. 7). The other three Balmer lines included in our spectra ($H\beta$, $H\gamma$ and $H\delta$) show a filled-in absorption line profile (see as an example the $H\beta$ line in Fig. 6). A strong emission in the Ca II H&K lines and a clear emission in the $H\epsilon$ line coming from both components is also detected. In addition, a clear emission above the continuum is observed in the core of the Ca II IRT absorption lines from both components (see Fig. 5 *b*).

Acknowledgements

This work was supported by the Universidad Complutense de Madrid, the Spanish Ministerio de Educación y Ciencia (MEC), Programa Nacional de Astronomía y Astrofísica under grant AYA2005-02750, and the "Comunidad de Madrid" under PRICIT project S-0505/ESP-0237 (ASTROCAM).

References

- Applegate J.H. 1992, *ApJ* 365, 621
- Barden S.C. 1985, *ApJ* 295, 162
- Cumming A. 2004, *MNRAS* 354, 1165
- Frasca A. & Lanza A.F. 2005, *ApJ* 429, 309
- Jeffries R.D., Bertram D. & Spurgeon R.D. 1995, *MNRAS* 276, 397
- Lanza A.F., Rodono M. & Rosner R. 1998, *MNRAS* 296, 893
- Lanza A.F. 2006, *MNRAS* 369, 1773
- Matese J.J. & Whirtmere D.P. 1983, *A&A* 117, L7
- Montes D., Fernández-Figueroa M.J., De Castro E. & Cornide M. 1995, *A&A* 294, 165
- Montes D., Fernández-Figueroa M.J., De Castro E. & Sanz-Forcada J. 1997, *A&A* 125, 263
- Montes D., Sanz-Forcada J., Fernández-Figueroa M.J., De Castro E. & Poncet A. 1998, *A&A* 330, 155

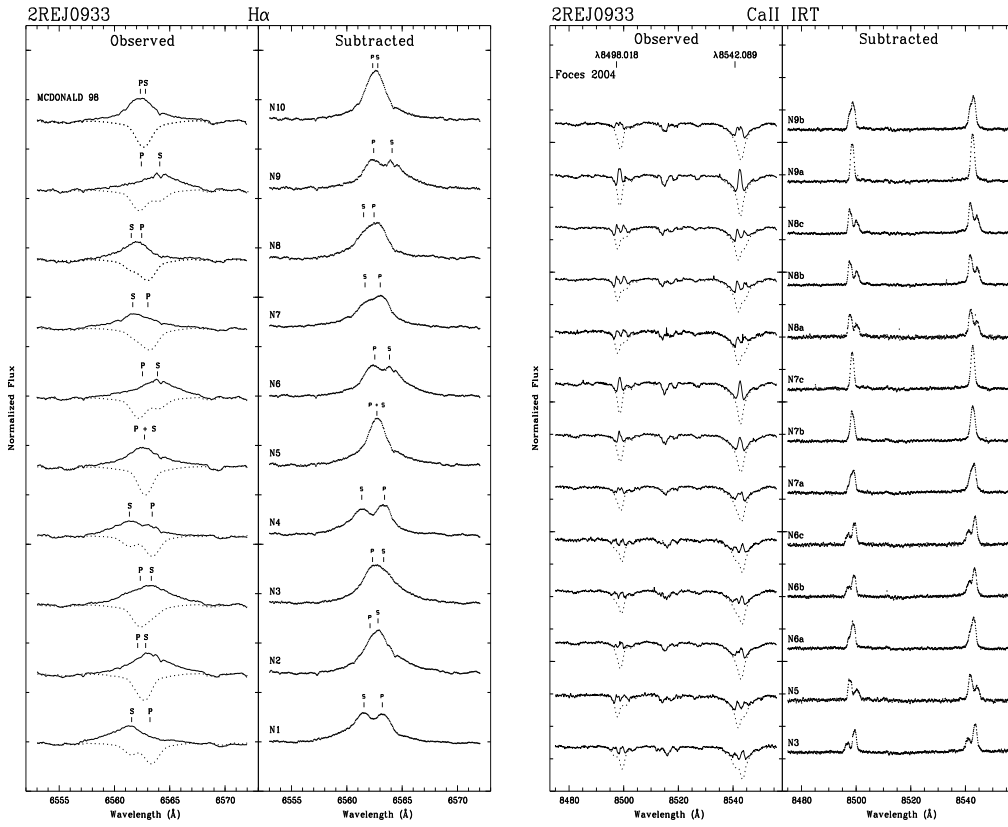


Figure 5. Spectra in H α line region (left figure) and Ca II IRT region (right figure) in FOCES04 observing run. The observed spectrum (solid-line) and the synthesized spectrum (dashed-line) are plotted in the left panel, and the subtracted spectrum (dotted line), in the right panel.

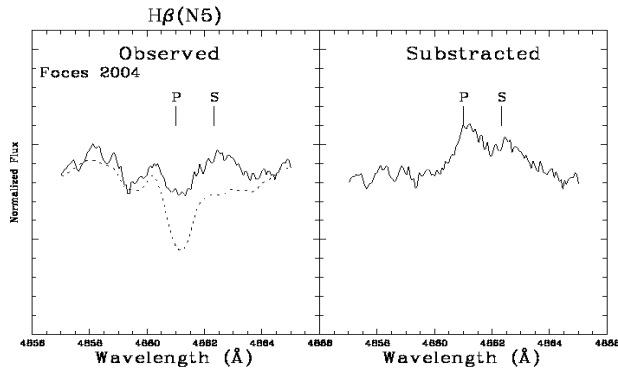


Figure 6. Observed spectrum (solid-line) and the synthesized spectrum (dashed-line) in the left panel, and the subtracted spectrum, in the right panel, in H β line region in FOCES04 observing run.

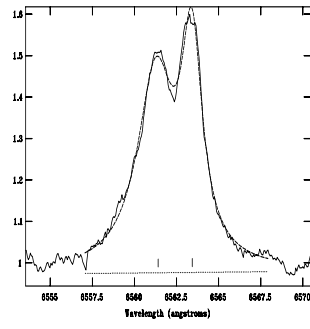


Figure 7. An example of the $H\alpha$ region fit in the subtracted spectrum by two Lorentzians.